

DEVELOPMENTAL-CELL-D-23-00194
By Cencer et al.

A Annotated sequence of Cdhr2-eGFP ssDNA donor (944 nt, sense strand):

Key: Cdhr2 Exon, LINKER, eGFP, 3'UTR, flanking genomic DNA

GCCCCTGACTGCAGTGCTCTCAGGAAGGTCGGCAGGTGCGAGCGAACAGCAGAAAAAG
AATCTGTCCTTCACCAACCCTGGCCTGGACACCACAGATCTGagcggcgaggtagcggagggtggc
agcATGGTGAGCAAGGGCGAGGAGCTGTTACCCGGGGTGGTGCCCATCTGGTCGAGCTG
GACGGCGACGTAAACGGCCACAAGTTCAGCGTGTCCGGCGAGGGCGAGGGCGATGCCAC
CTACGGCAAGCTGACCCTGAAGTTCATCTGCACCACCGCAAGCTGCCCGTGCCCTGGCC
CACCTCGTGACCACCCTGACCTACGGCGTGAGTGCTTACGCCGCTACCCCGACCACAT
GAAGCAGCAGACTTCTTCAAGTCCGCCATGCCGAAGGCTACGTCCAGGAGCGCACCAT
CTTCTTCAAGGACGACGGCAACTACAAGACCCGCGCCGAGGTGAAGTTCGAGGGCGACA
CCCTGGTGAACCGCATCGAGCTGAAGGGCATCGACTTCAAGGAGGACGGCAACATCCTG
GGCACAAGCTGGAGTACAACACTACAACAGCCACAACGTCTATATCATGGCCGACAAGCAG
AAGAACGGCATCAAGGTGAACCTCAAGATCCGCCACAACATCGAGGACGGCAGCGTGCAG
CTCGCCGACCACTACCAGCAGAACACCCCATCGGCGACGGCCCGTGTCTGTGCCCGA
CAACCACTACCTGAGCACCCAGTCCGCCCTGAGCAAAGACCCCAACGAGAAGCGCGATCA
CATGGTCTGTGAGTTCGTGACCGCCGCGGGATCACTCTCGGCATGGACGAGCTGTA
CAAGTGA CGGAGCCTGTCATTCTTCGAGCTCAAACCGTACTGTCTGCCCTCCCCTAAAAATA
TAATATATGGCCTTGCTTGTCAATCATAgacaagagtgggga

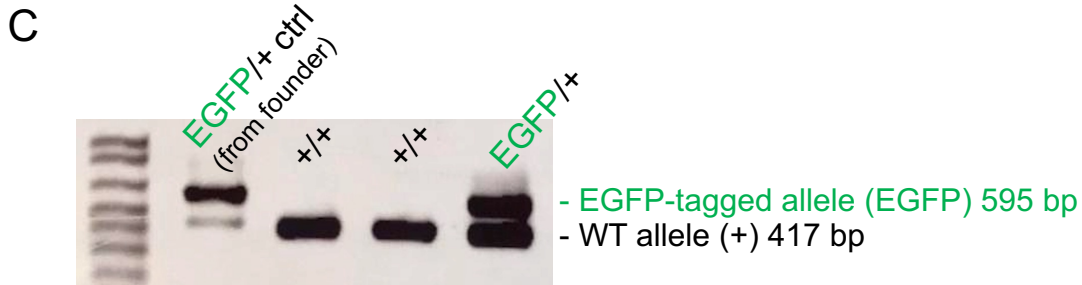
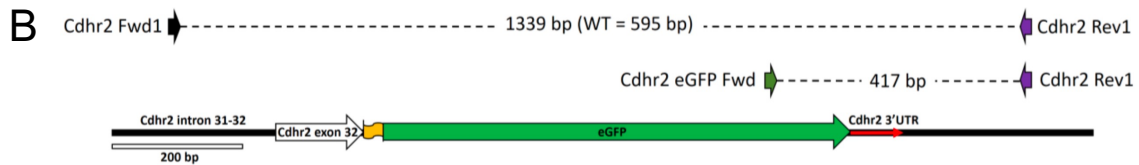


Figure S1, related to Figure 4: Strategy and validation of the CDHR2-EGFP knock-in mouse model. (A) Endogenous tagging strategy used to insert EGFP (green text) at the 3' end of mouse *CDHR2* allele (black text) in C57Bl/6N mice. (B) PCR strategy to screen for the presence of EGFP-tagged *CDHR2*. (C) Representative PCR outcomes showing bands for control (*CDHR2*^{+/+}) and heterozygous (*CDHR2*^{EGFP/+}) *CDHR2*-EGFP mice.

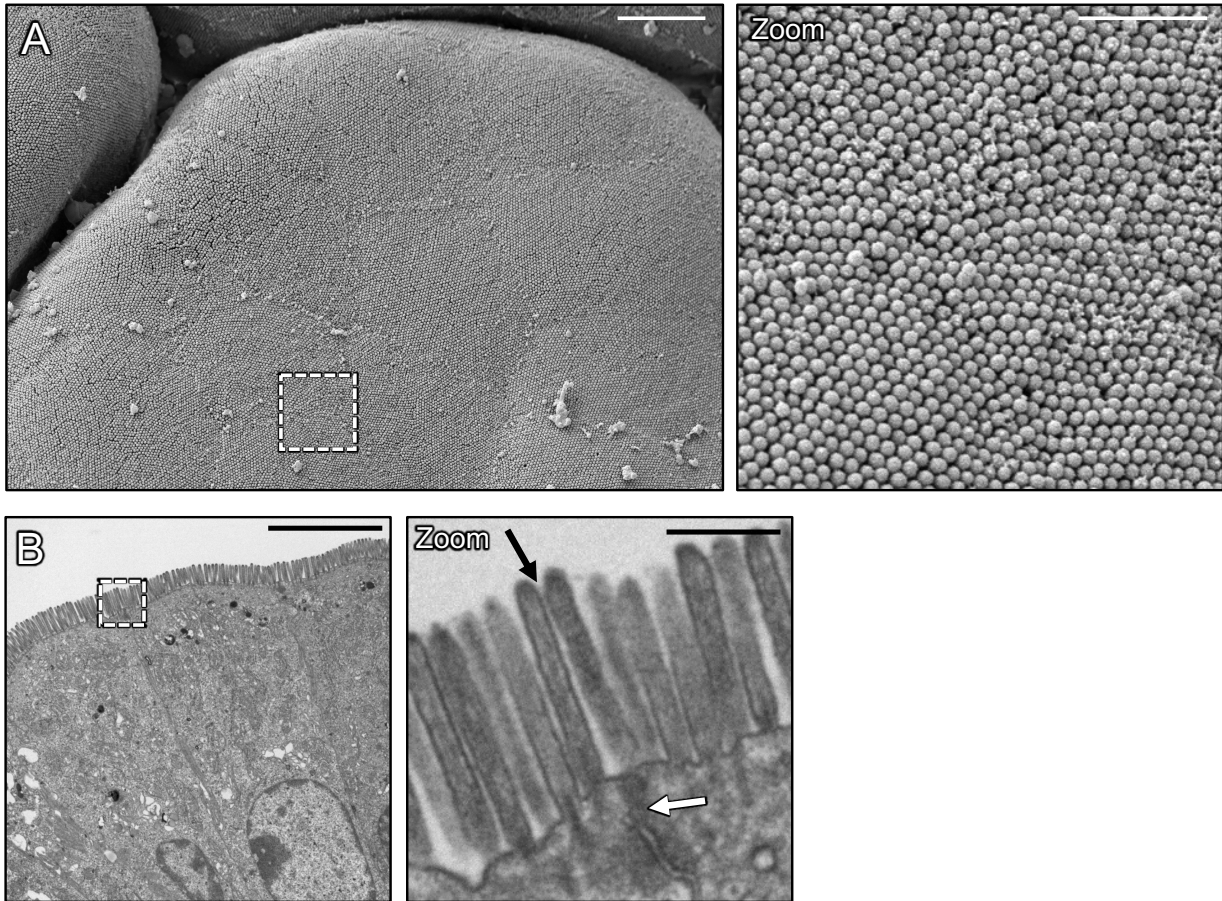


Figure S2: Mature villus enterocytes cells exhibit continuous packing of microvilli across cell junctions, related to Figure 4. (A) SEM of mouse small intestine showing an *en face* view of microvilli on neighboring enterocytes. The dashed box represents a zoom of a single enterocyte cell and its neighbors. (B) Transmission electron micrograph (TEM) of mouse small intestine showing a lateral view of microvilli. Dashed box represents the zoom of a cell-cell junction (white arrow) with neighboring cell microvilli appearing continuous across the interface (black arrow). Scale bars: 4 μm (A), 1 μm (A, zoom), 5 μm (B), 500 nm (B, zoom).

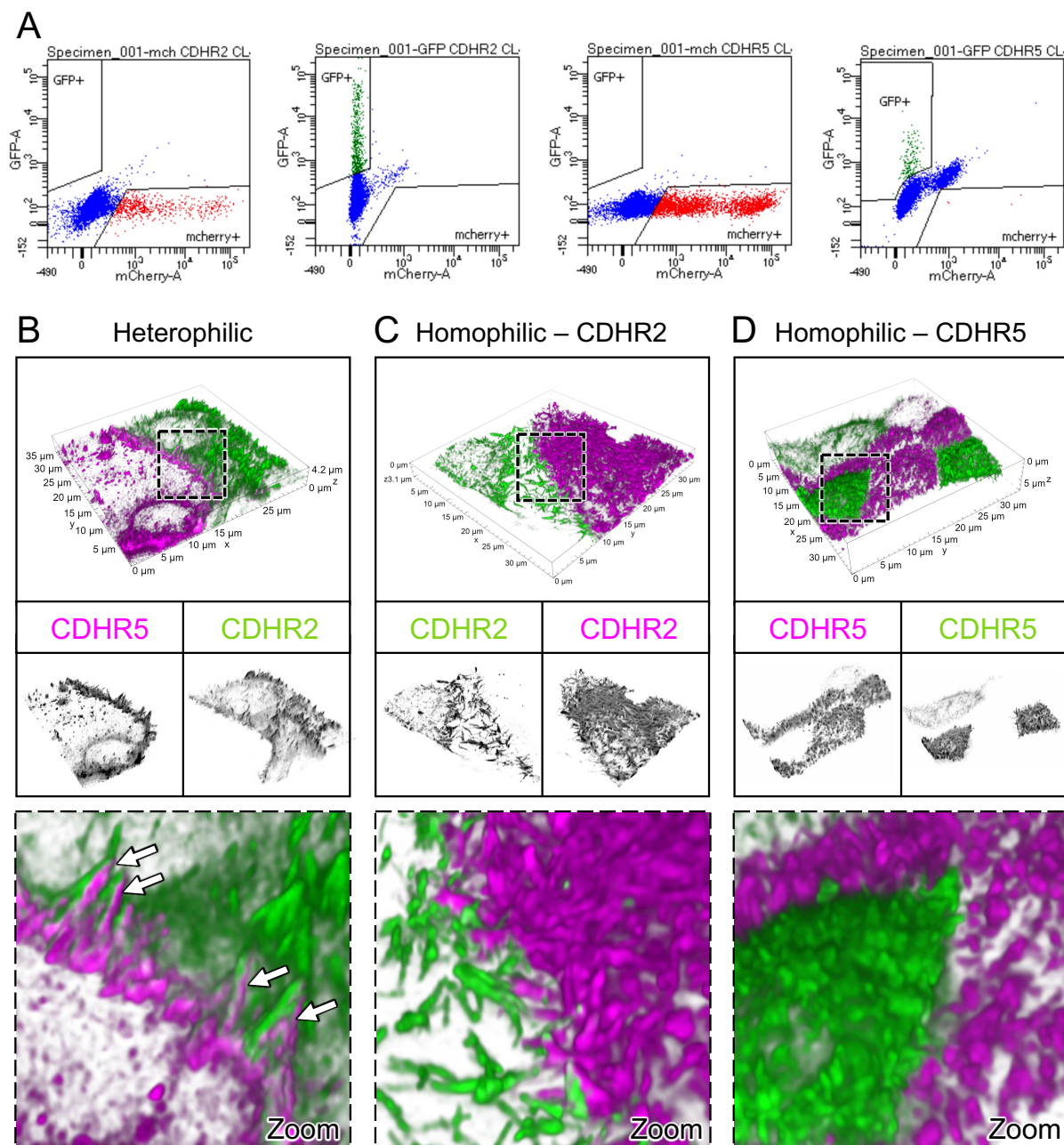


Figure S3: High-resolution imaging of adhesion complex interfaces in mixed CL4 cell populations, related to Figure 5. (A) FACS profiles of the four stable CL4 cell lines expressing C-terminal mCherry or EGFP tagged CDHR2 or CDHR5 as marked on the top axis of the graph. 3D Volume SIM images of mixed **(B)** heterophilic; CDHR5-mCherry and CDHR2-EGFP, **(C)** homophilic; CDHR2-EGFP and mCherry-CDHR5, and **(D)** homophilic; CDHR5-mCherry and CDHR5-EGFP CL4 cells. Dashed boxes outlined in B-D represent zooms shown in bottom panel, respectively. White arrows in zoom under (B) point to instances of robust microvilli alignment at cell margins, which are absent in the homophilic mixing scenarios. Scaled as marked.

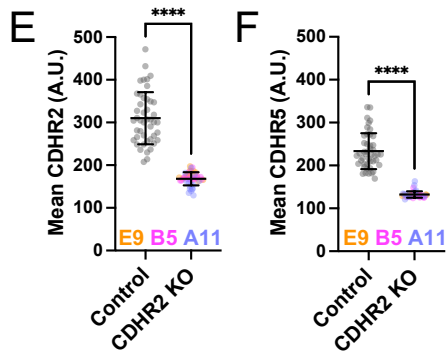
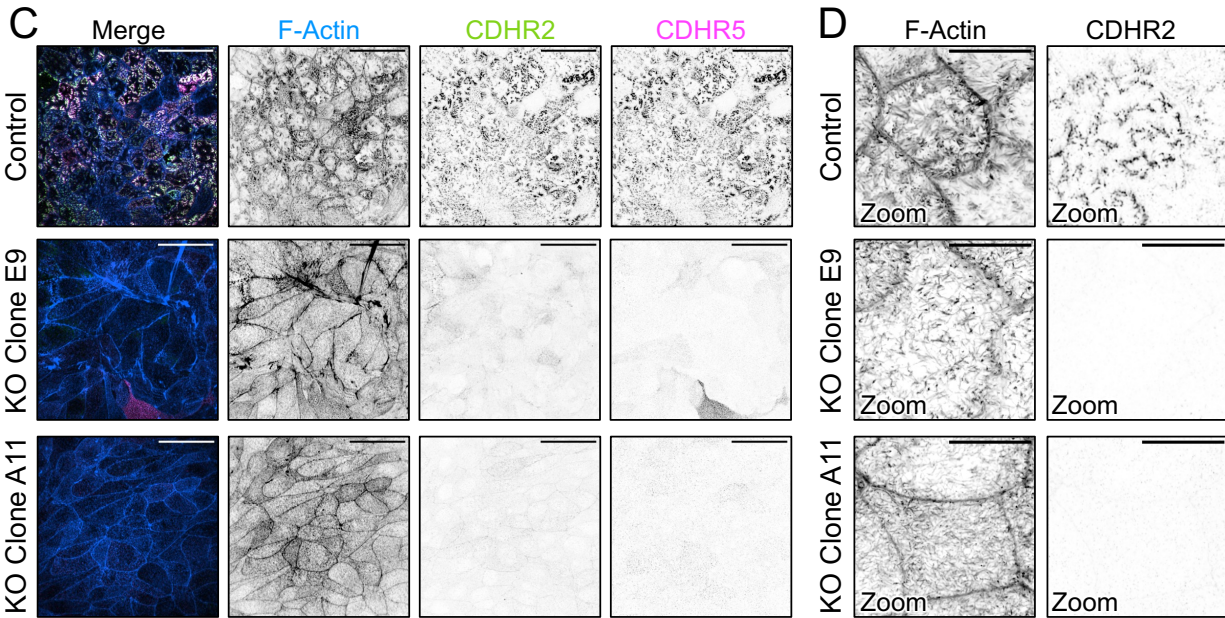
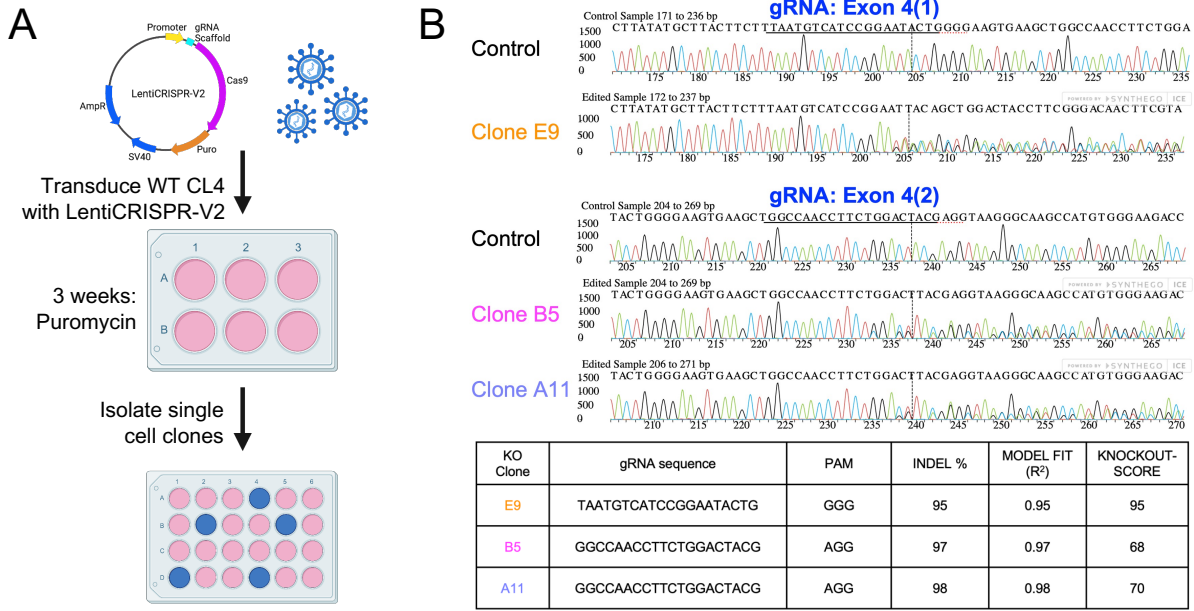
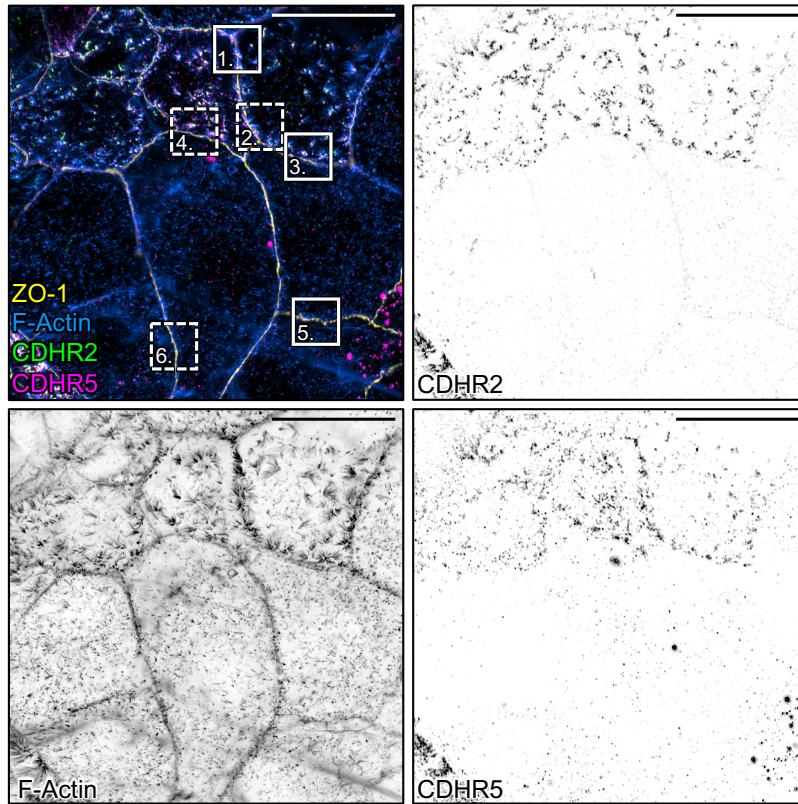


Figure S4: Generation and validation of CDHR2 KO CL4 cells, related to STAR Methods. (A) Schematic depicting the lentiCRISPRv2 system. The plasmid contains a

guide RNA (gRNA) scaffold, Cas9 enzyme, and puromycin selection marker. gRNA sequences (**B, table**) targeting Exon 4 of the CL4 porcine CDHR2 genomic region were cloned into the lentiCRISPRv2 plasmid. An empty lentiCRISPRv2 plasmid, with no added gRNA but still containing Cas9 machinery, was used as the “Control”. WT CL4 cells were transduced with CRISPR virus containing either of the two gRNA sequences and selected with puromycin. Single clones of selected cells were isolated and expanded into clonal “KO” populations. (**B**) Genomic DNA was extracted from the clones and PCR was used to generate a region spanning exons 4 and 5 of CDHR2. Trace files of each clone and the control cells were analyzed with the Synthego Inference of CRISPR Edits (ICE) tool [57]. (**C**) W1 spinning disc confocal MaxIP images of Control, CDHR2 KO Clone “E9”, and Clone “A11” stained for F-Actin (blue), CDHR2 (green), and CDHR5 (magenta). (**D**) Zooms from laser scanning confocal images of the same samples shown in (C) at a higher magnification showing the lack of microvillar clustering in KO clones. (**E**) Mean CDHR2 intensities of Control vs. CDHR2 KO clones. (**F**) Mean CDHR5 intensities of Control vs. CDHR2 KO clones. $n = 45$ total 60X imaged control fields and $n = 15$ 60X fields of each KO clone, total of $n = 45$ KO fields. Unpaired t-test; **** $p \leq 0.0001$. Error bars represent mean \pm SD. Scale bars: 40 μm (C), 10 μm (D).

A Control/KO Clone B5



B Ctrl/Ctrl Ctrl/KO KO/KO

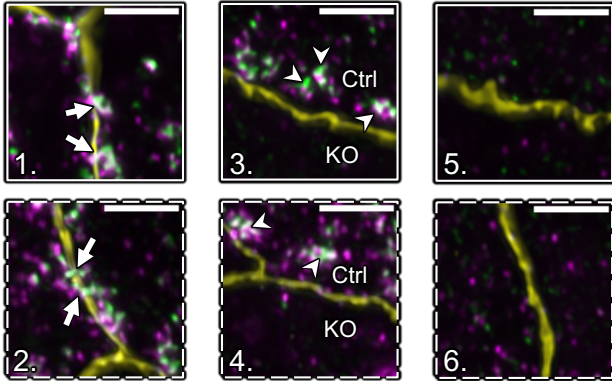


Figure S5: CDHR2 is required for transjunctional clustering of microvilli, related to Figure 5. (A) Laser scanning confocal MaxIP image of mixed cells stained for ZO-1 (yellow), CDHR2 (green), CDHR5 (magenta), and F-actin (blue). The solid and dashed boxes represent zooms, as numbered. **(B)** Control/Control (Ctrl/Ctrl) cell interfaces show clear clustering across ZO-1 marked junctions (zooms 1 and 2, white arrows) while Ctrl/KO interfaces demonstrate limited transjunctional clustering (zooms 3 and 4). Ctrl cells at Ctrl/KO interfaces still exhibit clustering (white arrowheads). KO/KO interfaces demonstrate little to no clustering at cell margins (zooms 5 and 6). Scale bars: 20 μ m (A), 3 μ m (B).

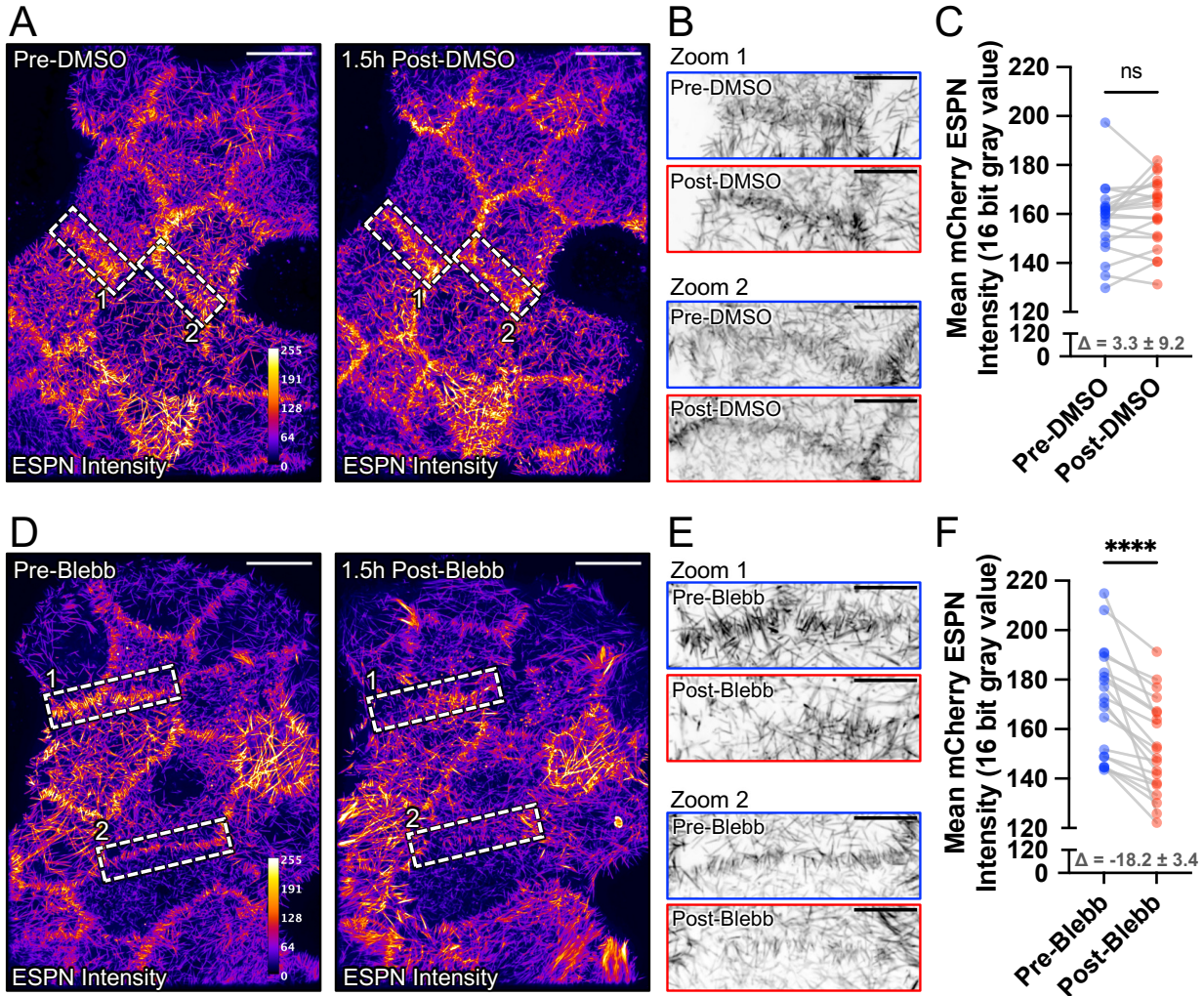


Figure S6: Myosin-2 dependent contractility stabilizes transjunctional clustering of microvilli, related to Figure 7. (A) Fire LUT intensity profile of the mCherry-ESPN channel Pre- and 1.5 hr Post-DMSO control treatment. (B) Zooms from the dashed boxes on (A) as marked showing inverted ESPN channel Pre- and 1.5 hr Post-DMSO. (C) Mean mCherry-ESPN intensities (16-bit gray values) of paired cell-cell interfaces Pre- and 1.5 hr Post-DMSO treatment; mean signal $\Delta = 3.3 \pm 9.2$. (D) Fire LUT intensity profile of the mCherry-ESPN channel Pre- and 1.5 hr Post-blebbistatin (20 μ M) addition. (E) Zooms from the dashed boxes on (D) as marked showing inverted ESPN channel Pre- and 1.5 hr Post-blebbistatin. (F) Mean mCherry-ESPN intensities (16-bit gray values) of paired cell-cell interfaces Pre- and 1.5 hr Post-blebbistatin treatment; error bars represent mean \pm SD; mean signal $\Delta = -18.2 \pm 3.4$. $n = 20$ pairs of linescans drawn along cell-cell interfaces for each treatment; paired t-test non-significant (ns) and **** $p \leq 0.0001$. Scale bars: 20 μ m (A,D), 10 μ m (B,E).